



## SHORT COMMUNICATION

# Plasmalemmal pH-Gradients in Drug-Sensitive and Drug-Resistant MCF-7 Human Breast Carcinoma Xenografts Measured by $^{31}\text{P}$ Magnetic Resonance Spectroscopy

Natarajan Raghunand,\* Maria I. Altbach,† Robert van Sluis,\* Brenda Baggett,\*  
Charles W. Taylor,‡ Zaver M. Bhujwalla§ and Robert J. Gillies\*||

DEPARTMENTS OF \*BIOCHEMISTRY, †RADIOLOGY, AND ‡INTERNAL MEDICINE, UNIVERSITY OF ARIZONA HEALTH SCIENCES CENTER, TUCSON, AZ 85724-5042; AND §DEPARTMENT OF RADIOLOGY, JOHNS HOPKINS SCHOOL OF MEDICINE, BALTIMORE, MD 21205, U.S.A.

**ABSTRACT.**  $^{31}\text{P}$  Magnetic resonance spectroscopy (MRS) was employed to investigate tumor pH in xenografts of drug-sensitive and drug-resistant MCF-7 human breast carcinoma cells. Measured extracellular pH values were found to be lower than the intracellular pH in all three tumor types investigated. The magnitude of this acid-outside plasmalemmal pH gradient increased with increasing tumor size in tumors of two drug-resistant variants of MCF-7 cells, but not in tumors of the parent (drug-sensitive) cells. The partitioning of weak-base or weak-acid drug molecules across the plasma membrane of a tumor cell is dependent upon the acid-dissociation constant ( $\text{pK}_a$ ) of the drug as well as the plasmalemmal pH gradient. A large acid-outside pH gradient, such as those seen in MCF-7 xenografts, can exert a protective effect on the cell from weak-base drugs such as anthracyclines and *Vinca* alkaloids, which have  $\text{pK}_a$  values of 7.5 to 9.5. The possibility of enhancing the therapeutic efficacy of weak-base drugs by dietary or metabolic manipulation of the extracellular pH, in order to reduce or reverse the plasmalemmal pH gradient, deserves investigation. *BIOCHEM PHARMACOL* 57;3:309–312, 1999. © 1998 Elsevier Science Inc.

**KEY WORDS.** MCF-7; breast carcinoma; xenograft; tumor pH;  $^{31}\text{P}$  magnetic resonance spectroscopy; 3-aminopropylphosphonate

Combination chemotherapy of breast cancer and other cancers usually involves the use of at least one partially ionizable drug species [1]. The partitioning of weak-base or weak-acid drug molecules across the plasma membrane of a tumor cell is dependent upon the  $\text{pK}_a$  of the drug as well as the plasmalemmal pH gradient. A large acid-outside pH gradient can exert a protective effect upon the cell from weak-base drugs such as anthracyclines and *Vinca* alkaloids, which have  $\text{pK}_a$  values of 7.5 to 9.5 [2–5]. The pH of tissues, including tumors, has been measured most commonly by the use of microelectrodes [6]. The pH thus measured is generally a combined measurement of the pH of interstitial fluid, and fluid and blood from damaged cells and capillaries. The invasive nature of microelectrodes and the uncertainty as to the nature of the interrogated fluid space complicate their use. In contrast,  $^{31}\text{P}$  MRS can be

employed to non-invasively, and simultaneously, measure  $\text{pH}_i$  from the chemical shift of endogenous inorganic phosphate [7] and  $\text{pH}_e$  from the chemical shift of exogenous 3-APP [8]. We have employed  $^{31}\text{P}$  MRS to investigate differences in the steady-state plasmalemmal pH gradients in xenografts of drug-sensitive and drug-resistant MCF-7 human breast carcinoma cells. The  $\text{pH}_e$  and  $\text{pH}_i$  of all cell lines decreased with increasing tumor size. However, the ( $\text{pH}_i - \text{pH}_e$ ) gradient was observed to increase with increasing tumor size only in tumors of two drug-resistant variants of MCF-7 cells, and not in tumors of the parent (drug-sensitive) cells. Implications of an acid-outside pH gradient for chemotherapy with weak-base drugs are discussed.

## MATERIALS AND METHODS

### Cells and Animals Used

MCF-7/S cells were obtained from the Michigan Cancer Foundation. MCF-7 cells resistant to mitoxantrone (MCF-7/Mitox) and doxorubicin (MCF-7/D40) were generated by sequential culturing in increased concentrations of mitoxantrone and doxorubicin, respectively [9]. SCID mice were obtained from the University of Arizona SCID mouse resource. Cells were implanted in the mammary fat pads of

|| Corresponding author: Dr. Robert J. Gillies, Department of Biochemistry, University of Arizona Health Sciences Center, 1501 North Campbell Ave., Tucson, AZ 85724-5042. Tel. (520) 626-5050; FAX (520) 626-2110; E-mail: gillies@u.arizona.edu

¶Abbreviations: 3-APP, 3-aminopropylphosphonate; MRS, magnetic resonance spectroscopy; NTP, nucleoside triphosphate;  $\text{pH}_e$ , extracellular pH;  $\text{pH}_i$ , intracellular pH;  $\text{pK}_a$ , acid-dissociation constant; and SCID, severe combined immune-deficient.

Received 3 June 1998; accepted 2 September 1998.

6- to 7-week-old female SCID mice as a suspension of  $5 \times 10^6$  cells in 0.05 mL of Hanks' balanced salt solution containing 50% Matrigel (Collaborative Research). As these cells are estrogen-dependent,  $17\beta$ -estradiol pellets (0.25 mg, 21-day release; or 0.75 mg, 60-day release; Innovative Research of America) were implanted subcutaneously in the shoulder region of the mice by means of a 12-gauge trocar (Innovative Research) 2 days prior to tumor inoculation. In the case of the 21-day release pellets, a new pellet was implanted every 3 weeks, as necessary.

### *In vivo* MRS

Tumors were allowed to grow for 3–8 weeks to volumes of 150–1500 mm<sup>3</sup>, as estimated by external measurements of the tumor. Tumor volumes were calculated from orthogonal measurements of the external dimensions of tumors using the formula (width)<sup>2</sup>  $\times$  length/2 [10]. Prior to MRS, the mice were anesthetized with a combination of ketamine (72 mg/kg), xylazine (6 mg/kg), and acepromazine (6 mg/kg). A 3/4 in., 24-gauge catheter (Elf Sanofi Inc.) connected to a 1.58 mm i.d. polyethylene tube (Becton Dickinson) long enough to extend out of the magnet was inserted into the intraperitoneal cavity of the anesthetized animal. 3-APP was obtained from the Sigma Chemical Co. A solution of 3-APP (0.15 to 0.3 mL, 128 mg/mL, pH 7.4) could be remotely injected into the mouse at the appropriate time before spectroscopy via the i.p. catheter. All *in vivo* measurements were performed at 4.7 Tesla (T) on a Bruker Biospec spectrometer/imager. The mouse was immobilized on a home-built probe, with the whole tumor placed inside a 3-turn solenoid radiofrequency (rf) coil of appropriate diameter—8, 12, or 17 mm—tunable to <sup>1</sup>H or <sup>31</sup>P. Body temperature was maintained by a circulating water blanket placed under the immobilized mouse. Unlocalized <sup>31</sup>P MR spectra were acquired using 20–45° pulses with repetition times of 500–1000 msec. Volume-selective <sup>31</sup>P spectra were acquired using either VSEL, a double-refocused spin-echo implementation of the VOSY pulse sequence [11] provided by Bruker Medizintechnik, or the ISIS sequence [12]. Scout images of the tumors were acquired prior to localized spectroscopy, to guide voxel placement. VSEL spectra were acquired using 764  $\mu$ sec slice-selective hermitian rf pulses (corresponding to 80 ppm in the <sup>31</sup>P MR spectrum), an echo time of 11 msec, and a repetition time of 1200 msec. ISIS spectra were acquired with adiabatic slice-selective and excitation pulses repeated every 10–12 sec, using a gradient strength of 75 mT/m. In all cases, a dwell time of 62.5  $\mu$ sec was employed, and 8192 data points were collected. Transients were averaged for 10–30 min. The large spectral widths employed resulted in up to a 1-mm difference in the positioning of the voxel containing either  $\alpha$ -NTP or 3-APP, and the voxel containing the central frequency. This chemical shift artifact was not corrected for, but voxel sizes and placement were chosen so as to minimize the contribution of signal arising from the mouse body wall, while covering as much of the tumor as possible.

### *pH* Calibration of Spectral Peaks

<sup>31</sup>P MR time-domain data were processed by exponential multiplication followed by Fourier transformation. Chemical shifts of 3-APP and inorganic phosphate were calibrated to the  $\alpha$  peak of NTP (set to  $-10.05$  ppm). Titration curves reported elsewhere for the pH-dependencies of the chemical shifts of 3-APP [13, \*] and inorganic phosphate [14] were used to calculate pH<sub>e</sub> and pH<sub>i</sub>, respectively, from each <sup>31</sup>P MR spectrum. The intensity of each 3-APP peak was corrected for the non-linearity of the titration curve prior to assigning a pH value to the chemical shift of the top of the peak [15]. Figure 1 shows a representative <sup>31</sup>P MR spectrum of an MCF-7/S tumor obtained using the ISIS sequence.

### Statistical Analyses

Tumor pH<sub>e</sub> and pH<sub>i</sub> were obtained from <sup>31</sup>P MR spectra of several MCF-7/S, MCF-7/D40, and MCF-7/Mitox tumors. A linear regression analysis was performed for data sets from each tumor type, in order to determine the nature of the relationship between tumor pH<sub>e</sub> (or pH<sub>i</sub>) and tumor volume. The values and 95% confidence intervals for the first-order regression parameters were calculated using Sigmatstat (Jandel Corp.).

## RESULTS AND DISCUSSION

### <sup>31</sup>P MR Spectrum

Figure 1 shows a representative <sup>31</sup>P MR spectrum of a 610 mm<sup>3</sup> MCF-7/S tumor, obtained from an  $8 \times 8 \times 8$  mm<sup>3</sup> voxel within the tumor. pH<sub>e</sub> and pH<sub>i</sub> were calculated from the chemical shifts of the 3-APP and inorganic phosphate peaks, respectively, as described in Materials and Methods.

### Variation in pH<sub>e</sub> and pH<sub>i</sub> with Tumor Size

Panels a–c of Fig. 2 display the tumor pH<sub>e</sub> and pH<sub>i</sub> measured from localized and unlocalized <sup>31</sup>P MR spectra of three different tumor types, as a function of tumor volume. Also displayed are the results of first-order linear regression curve fits for each data set. Table 1 shows the values and the 95% confidence intervals for the fitted slopes, obtained from a linear regression analysis of each data set. The data clearly show that tumor pH<sub>e</sub> and pH<sub>i</sub> decrease with increasing tumor size.

### Variation of Plasmalemmal (pH<sub>i</sub>–pH<sub>e</sub>) Gradient with Tumor Volume

The first-order fitted lines shown in Fig. 2a indicate that for the drug-sensitive MCF-7/S tumors, the magnitude of the

\* Raghunand N, Aiken NR, Bhujwala ZM and Gillies RJ, Measurement of extracellular pH *in vivo* using 3-aminopropylphosphonate: Deconvolution of T<sub>2</sub>\* effects. In: *Proceedings of the International Society for Magnetic Resonance in Medicine*, Vol. 2, p. 1111, 1996.

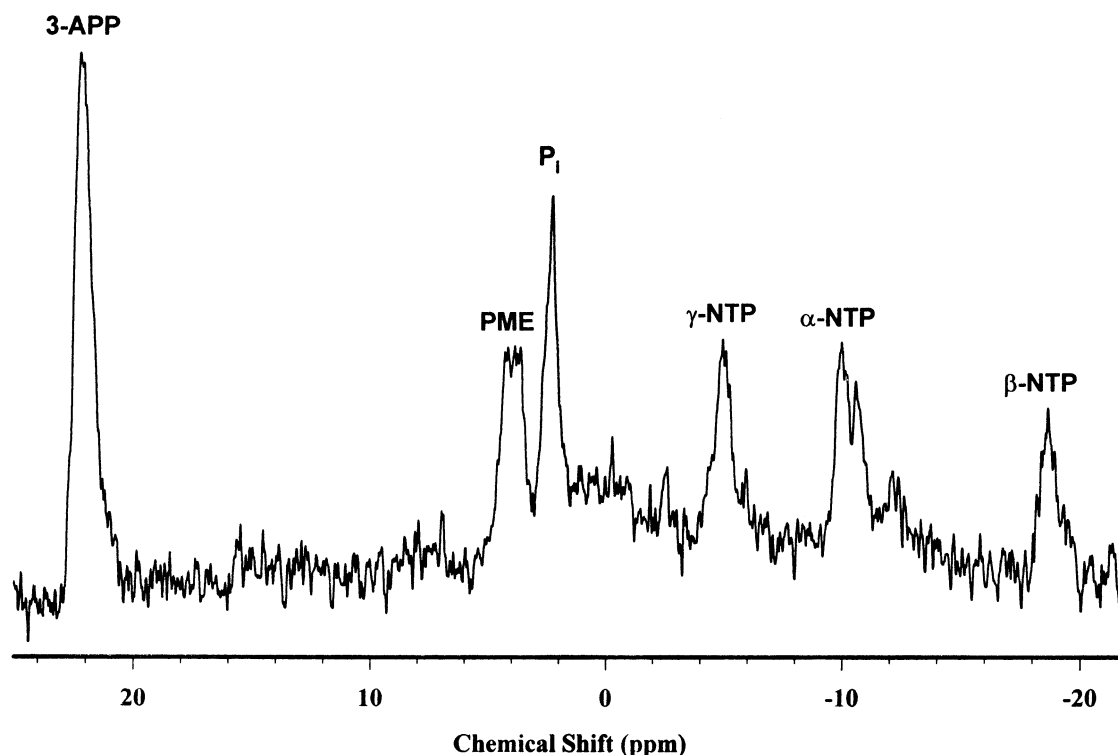


FIG. 1.  $^{31}\text{P}$  MR ISIS spectrum acquired from an  $8 \times 8 \times 8 \text{ mm}^3$  voxel placed on a  $610 \text{ mm}^3$  MCF-7/S tumor. Adiabatic excitation pulses were used to minimize artifacts arising from non-uniform spatial excitation; 8192 data points were collected over a spectral window of 8000 Hz, from a total of 184 averages with a recycle delay of 10.5 sec. An exponential line-broadening factor of 5 Hz was applied to the time-domain signal prior to Fourier transformation. P<sub>i</sub>, inorganic phosphate; NTP, nucleoside triphosphate; and PME, phosphomonoesters.  $\text{pH}_{3\text{-APP}} = 7.11$ ,  $\text{pH}_{\text{P}_i} = 7.17$ .

( $\text{pH}_i - \text{pH}_e$ ) gradient changed little with increasing tumor volumes. The  $\text{pH}_i$  dropped concomitantly with the drop in  $\text{pH}_e$ . The overlapping 95% confidence intervals for the slopes of the  $\text{pH}_e$  and  $\text{pH}_i$  data sets for the MCF-7/S tumors (Table 1) verify that the ( $\text{pH}_i - \text{pH}_e$ ) gradient was not altered significantly. From panels b and c of Fig. 2, it can be

seen that the fitted lines are divergent for the  $\text{pH}_i$  and  $\text{pH}_e$  values of MCF-7/D40 and MCF-7/Mitox tumors. Thus, for these tumors, the magnitude of the ( $\text{pH}_i - \text{pH}_e$ ) gradient increased as the tumors grew. The 95% confidence intervals for the fitted slopes for the  $\text{pH}_e$  and  $\text{pH}_i$  data sets from both MCF-7/D40 and MCF-7/Mitox tumors did not overlap

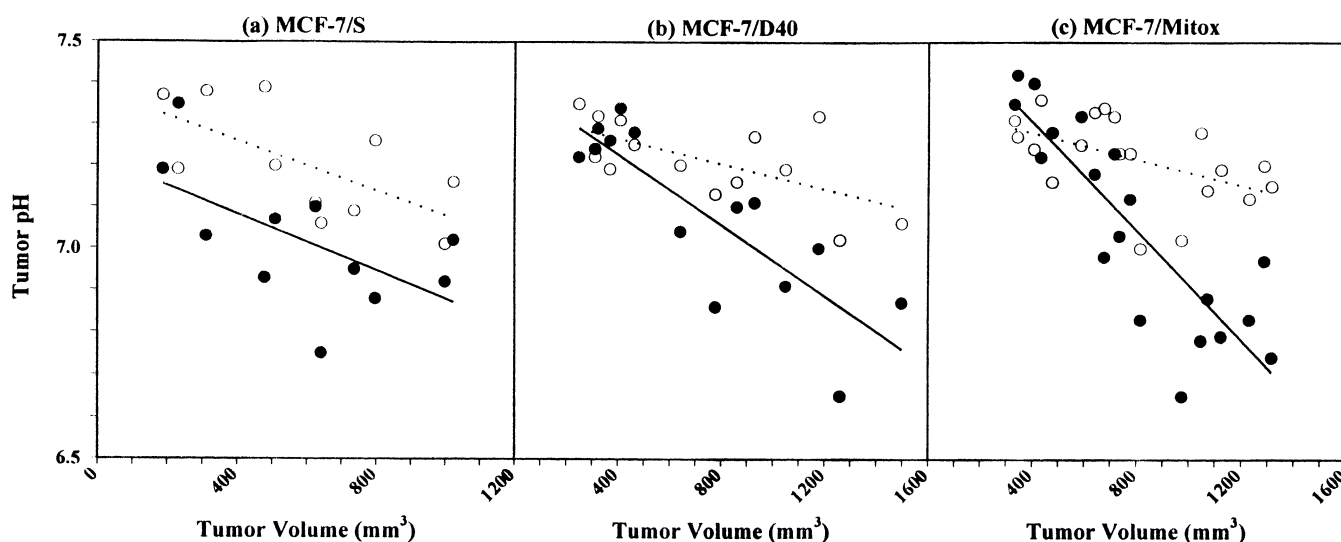


FIG. 2. Variation in  $\text{pH}_i$  and  $\text{pH}_e$  with tumor size. (a) MCF-7/S tumors, (b) MCF-7/D40 tumors, and (c) MCF-7/Mitox tumors. Key: (●)  $\text{pH}_e$  data, (○)  $\text{pH}_i$  data, (—)  $\text{pH}_e$  linear regression, and (···)  $\text{pH}_i$  linear regression.

**TABLE 1.** Slopes and 95% confidence intervals for the tumor pH versus the tumor volume data sets shown in Fig. 2

Data set	Fitted slope ( $10^{-4}$ pH units/mm <sup>3</sup> )	95% Confidence interval ( $10^{-4}$ pH units/mm <sup>3</sup> )
MCF-7/S, pH <sub>e</sub>	-3.4	-1.9 to -4.9
MCF-7/S, pH <sub>i</sub>	-3.0	-1.8 to -4.2
MCF-7/D40, pH <sub>e</sub>	-4.3	-3.5 to -5.0
MCF-7/D40, pH <sub>i</sub>	-1.5	-0.98 to -2.1
MCF-7/Mitox, pH <sub>e</sub>	-6.6	-5.6 to -7.5
MCF-7/Mitox, pH <sub>i</sub>	-1.6	-0.93 to -2.2

(Table 1), indicating that the slopes of the pH<sub>e</sub> and pH<sub>i</sub> regressions for these two tumor types were significantly different. Furthermore, the pH<sub>e</sub> slope for MCF-7/Mitox tumors was significantly steeper than that for MCF-7/D40 tumors.

It is thus clear that (i) a positive (pH<sub>i</sub>-pH<sub>e</sub>) gradient exists in tumors of all three variants of MCF-7 cells, and (ii) the magnitude of this gradient increases with increasing tumor volume in the two drug-resistant variants, but not the drug-sensitive parent tumor type. A pH gradient in this direction may confer a measure of protection to the tumors from weak-base drugs like doxorubicin and mitoxantrone, by partial exclusion of the drugs from the cytosol [2-5]. This would be a form of "physiological" drug resistance, as distinct from the better characterized "biochemical" drug resistance observed, for example, in cells expressing the P-glycoprotein drug pump (reviewed in Ref. 16). The increased magnitude of the plasmalemmal pH gradient in MCF-7/D40 and MCF-7/Mitox tumors at the larger tumor sizes may partially explain why the large tumors are refractory to drug therapy (unpublished results). While such a pH gradient would seem to favor the use of weak-acid drugs such as chlorambucil, these are not commonly used. The possibility of enhancing the therapeutic efficacy of commonly used weak-base drugs by dietary or metabolic manipulation of pH<sub>e</sub> in order to reduce or reverse the plasmalemmal pH gradient deserves investigation.

*This work was supported by the U.S. Army Breast Cancer Research Program, Grant DAMD17-94-J-4368*

## References

1. Taylor CW, Dalton WS, Mosley K, Dorr RT and Salmon SE, Combination chemotherapy with cyclophosphamide, vincristine, adriamycin, and dexamethasone (CVAD) plus oral quinine and verapamil in patients with advanced breast cancer. *Breast Cancer Res Treat* **42**: 7-14, 1997.
2. Tannock IF and Rotin D, Acid pH in tumors and its potential for therapeutic exploitation. *Cancer Res* **49**: 4373-4384, 1989.
3. Roepe PD, Analysis of the steady-state and initial rate of doxorubicin efflux from a series of multidrug-resistant cells expressing different levels of P-glycoprotein. *Biochemistry* **31**: 12555-12564, 1992.
4. Simon S, Roy D and Schindler M, Intracellular pH and the control of multidrug resistance. *Proc Natl Acad Sci USA* **91**: 1128-1132, 1994.
5. Gerweck LE and Seetharaman K, Cellular pH gradient in tumor versus normal tissue: Potential for exploitation for the treatment of cancer. *Cancer Res* **56**: 1194-1198, 1996.
6. Wike-Hooley JL, Haveman J and Reinhold HS, The relevance of tumour pH to the treatment of malignant disease. *Radiother Oncol* **2**: 343-366, 1984.
7. Stubbs M, Bhujwala ZM, Tozer GM, Rodrigues LM, Maxwell RJ, Morgan R, Howe FA and Griffiths JR, An assessment of <sup>31</sup>P MRS as a method of measuring pH in rat tumours. *NMR Biomed* **5**: 351-359, 1992.
8. Gillies RJ, Liu Z and Bhujwala Z, <sup>31</sup>P-MRS measurements of extracellular pH of tumors using 3-aminopropylphosphonate. *Am J Physiol* **267**: C195-C203, 1994.
9. Taylor CW, Dalton WS, Parrish PR, Gleason MC, Bellamy WT, Thompson FH, Roe DJ and Trent JM, Different mechanisms of decreased drug accumulation in doxorubicin and mitoxantrone resistant variants of the MCF7 human breast cancer cell line. *Br J Cancer* **63**: 923-929, 1991.
10. Taetle R, Rosen F, Abramson I, Venditti J and Howell S, Use of nude mouse xenografts as preclinical drug screens: *In vivo* activity of established chemotherapeutic agents against melanoma and ovarian carcinoma xenografts. *Cancer Treat Rep* **71**: 297-304, 1987.
11. Kimmich R and Hoepfel D, Volume-selective multipulse spin-echo spectroscopy. *J Magn Reson* **72**: 379-384, 1987.
12. Ordidge RJ, Bowley RM and McHale G, A general approach to selection of multiple cubic volume elements using the ISIS technique. *Magn Reson Med* **8**: 323-331, 1988.
13. McCoy CL, Parkins CS, Chaplin DJ, Griffiths JR, Rodrigues LM and Stubbs M, The effect of blood flow modification on intra- and extracellular pH measured by <sup>31</sup>P magnetic resonance spectroscopy in murine tumors. *Br J Cancer* **72**: 905-911, 1995.
14. Gillies RJ, Alger JR, den Hollander JA and Shulman RG, Intracellular pH measured by NMR: Methods and results. In: *Intracellular pH: Its Measurement, Regulation, and Utilization in Cellular Functions* (Eds. Nuccitelli R and Deamer DW), pp. 79-104. Alan R. Liss, New York, 1982.
15. Graham RA, Taylor AH and Brown TR, A method for calculating the distribution of pH in tissues and a new source of pH error from the <sup>31</sup>P-NMR spectrum. *Am J Physiol* **266**: R638-R645, 1994.
16. Gottesman MM and Pastan I, Biochemistry of multidrug resistance mediated by the multidrug transporter. *Annu Rev Biochem* **62**: 385-427, 1993.